

N O T I C E

THIS DOCUMENT HAS BEEN REPRODUCED FROM
MICROFICHE. ALTHOUGH IT IS RECOGNIZED THAT
CERTAIN PORTIONS ARE ILLEGIBLE, IT IS BEING RELEASED
IN THE INTEREST OF MAKING AVAILABLE AS MUCH
INFORMATION AS POSSIBLE

80-FM-11

JSC-16411

"Made available under NASA sponsorship
in the interest of early and wide dis-
semination of Earth Resources Survey
Program information and without liability
for any use made thereof."

Proximity Operations Analysis

(NASA-TM-81104) PROXIMITY OPERATIONS
ANALYSIS: RETRIEVAL OF THE SOLAR MAXIMUM
MISSION OBSERVATORY (NASA) 41 p
HC A03/MF A01

N80-28411

CSCL 22A

G3/16

Unclass
26416

Retrieval of the Solar Maximum Mission Observatory

Mission Planning and Analysis Division

April 1980

NASA

National Aeronautics and
Space Administration

Lyndon B. Johnson Space Center
Houston, Texas

80-FM-11

80FM11

JSC-16411

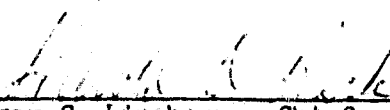
SHUTTLE PROGRAM

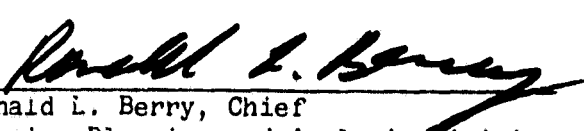
PROXIMITY OPERATIONS ANALYSIS

RETRIEVAL OF THE SOLAR MAXIMUM MISSION OBSERVATORY

By J. A. Yglesias
McDonnell Douglas Technical Services Co.

JSC Task Monitor: Michael Donahoo
Flight Planning Branch

Approved: 
Edgar C. Lineberry, Chief
Flight Planning Branch

Approved: 
Ronald L. Berry, Chief
Mission Planning and Analysis Division

Mission Planning and Analysis Division
National Aeronautics and Space Administration
Lyndon B. Johnson Space Center
Houston, Texas
April 1980

ACKNOWLEDGMENT

Simulations and analyses required to produce these data and results were performed and supplied by Jerry Yglesias of the McDonnell Douglas Technical Services Company of Houston.

CONTENTS

Section		Page
1.0	<u>SUMMARY</u>	1
2.0	<u>INTRODUCTION</u>	1
2.1	PURPOSE	2
2.2	PROXIMITY OPERATIONS TERMINOLOGY	2
2.2.1	<u>Local Vertical/Local Horizontal Coordinate System</u>	2
2.2.2	<u>Approach Techniques</u>	2
2.2.3	<u>Close-In Braking Techniques</u>	2
2.2.4	<u>Sun and Roll Angles</u>	3
2.2.5	<u>Onorbit Digital Autopilot</u>	3
2.2.6	<u>Universal Pointing Processor</u>	3
2.3	CANDIDATE FINAL APPROACH PROFILES	4
3.0	<u>DISCUSSION</u>	4
3.1	POTENTIAL PROBLEMS	4
3.2	METHODOLOGY	5
3.3	FINAL APPROACH PROFILES	6
3.3.1	<u>In-Plane Profile</u>	6
3.3.2	<u>Out-of-Plane Profile</u>	7
3.4	COMPARISONS	8
4.0	<u>SIMULATION RESULTS</u>	8
4.1	IN-PLANE RESULTS	8
4.2	OUT-OF-PLANE RESULTS	9
4.3	SIMULATION PLOTS	9
5.0	<u>CONCLUSIONS</u>	9
6.0	<u>RECOMMENDATIONS</u>	10
7.0	<u>REFERENCES</u>	11

IF ANY PAGE BLANK NOT FILMED

TABLES

Table		Page
I	ANALYSIS ASSUMPTIONS	12
II	IN-PLANE SIMULATION RESULTS	13
III	OUT-OF-PLANE SIMULATION RESULTS	14

FIGURES

Figure		Page
1	Local vertical/local horizontal coordinate system	15
2	Braking methods	16
3	Solar maximum mission observatory	17
4	SMM control axes	18
5	In-plane approach profile	19
6	Out-of-plane approach profile	20
7	Desired alinement prior to grapple	21
8	Geometry models for SMM configuration	22
9	Paper pilot logic	23
10	Flyaround and final approach for GF in orbital plane . . .	24
11	Two-phase flyaround	25
12	Automatic roll and manually centering SMM in COAS results in flyaround	26
13	One-phase flyaround	27
14	Approach chart (in-plane profile)	28
15	Torque impulse history (in-plane profile)	29
16	Propellant consumption (in-plane profile)	30
17	Approach chart (out-of-plane profile)	31
18	Torque impulse history (out-of-plane profile)	32
19	Propellant consumption (out-of-plane profile)	33
20	Third-person view (out-of-plane profile)	34

ACRONYMS

COAS	crew optical alignment sight
DAP	digital autopilot
GF	grapple fixture
LVLH	local vertical/local horizontal
POPIS	proximity operations/plume impingement simulation
PRCS	primary reaction control system
RMS	remote manipulator system
SMM	solar maximum mission
SVDS	space vehicle dynamics simulation
THC	translational hand controller
UPP	universal pointing processor

1.0 SUMMARY

Retrieval of the solar maximum mission (SMM) observatory is feasible in terms of Orbiter primary reaction control system (PRCS) plume disturbance of the SMM, Orbiter propellant consumed, and flight time required. Although digital simulations of the proposed final approach profiles demonstrate that these techniques will work, man-in-loop simulations will be required to validate these operational techniques before the verification process is complete.

Candidate approach and flyaround techniques have been developed that will allow the Orbiter to attain the proper alignment with the SMM for clear access to the grapple fixture (GF) prior to grappling. Because the SMM has very little control authority (approximately 14.8 pound-foot-seconds in two axes and rate-damped in the third) it will be necessary to inhibit all +Z (upfiring) PRCS jets on the Orbiter to avoid tumbling the SMM.

A profile involving a V-bar approach and an out-of-plane flyaround appears to be the best choice and is recommended at this time. The flyaround technique consists of aligning the +X-axes of the two vehicles parallel with each other and then flying the Orbiter around the SMM until the GF is in view. By using the automatic attitude control capabilities of the Orbiter digital autopilot (DAP) and universal pointing processor (UPP), the pilot's workload during the flyaround consists of keeping the SMM centered in the crew optical alignment sight (COAS) and maintaining a desired range and range rate by using translational hand controller (THC) deflections.

Finally, the out-of-plane flyaround technique proposed for SMM retrieval is applicable to any inertially stabilized payload. Also, the entire final approach profile could be considered as standard for most retrieval missions.

2.0 INTRODUCTION

The solar observatory, SMM, will perform a series of experiments coordinated by the Goddard Space Flight Center. It will be launched on a conventional Delta booster and then retrieved by the Shuttle. SMM is an actively controlled spacecraft, and in the remainder of this paper the feasibility of the SMM retrieval mission is addressed from a proximity operations viewpoint.

In this section, terms pertinent to proximity operations and this study are defined. Also, a brief overview of the candidate approach profiles is presented. Section 3 includes the problems that are specific to SMM, the methods and tools used in the profile design process, and finally a detailed discussion (including comparisons) of the various profiles that were simulated. In section 4, the simulation results (numerical and graphical data) are presented. These data lead to the conclusions and recommendations of sections 5.0 and 6.0, respectively. Finally, a list of references is given in section 7.0.

2.1 PURPOSE

The purpose of this study was to develop candidate approach profiles for SMM retrieval that would be acceptable in terms of plume impingement, propellant consumption, time, and pilot workload. Final recommendations would then be made based upon the comparisons of the various profiles.

2.2 PROXIMITY OPERATIONS TERMINOLOGY

2.2.1 Local Vertical/Local Horizontal Coordinate System

The local vertical/local horizontal (LVLH) system has its origin at the vehicle center of mass; Z_{LVLH} lies along the geocentric radius vector to the vehicle positive toward the center of the Earth, X_{LVLH} is aligned with the velocity vector, and Y_{LVLH} completes the right-handed system (fig. 1).

2.2.2 Approach Techniques

In this study three basic Orbiter approaches to the SMM were analyzed: R-bar, V-bar, and inertial.

For the R-bar approach, the Orbiter approaches along the Z_{LVLH} axis (radius vector). The primary advantage of this method is that "natural braking" because of gravity greatly reduces the amount of active braking (upfiring PRCS jet activity) necessary to null the range rate between the Orbiter and SMM. However, some of the propellant savings from "natural braking" is offset by increased X-jet firings to keep the Orbiter on the Z_{LVLH} axis.

For the V-bar approach, the Orbiter approaches along the X_{LVLH} axis (velocity vector). For this technique, very little propellant is required to keep the Orbiter on the X_{LVLH} axis; however, since there is no "natural braking," considerable active braking is required to null the range rate between the two vehicles. Active braking results in increased PRCS plume impingement on the payload.

For the inertial approach, the Orbiter approaches the payload along a vector fixed in inertial space. Although this technique is clear-cut, maintaining a range versus range-rate schedule can be difficult because of orbital mechanics effects.

2.2.3 Close-In Braking Techniques

The methods used to control the range rate of the Orbiter with respect to the payload greatly affect the amount of plume impingement imparted to the payload. The two techniques that were considered, normal-Z braking and low-Z braking, are shown in figure 2.

For normal-Z braking, three upfiring PRCS jets (one forward and two aft) are fired simultaneously. The combined 2600 pounds-force of thrust results in an

acceleration of about 0.4 fps^2 for a 200 000-pound Orbiter. This is the fastest and most efficient way to null the relative rates, but at ranges less than 500 feet, plume impingement on the payload is a potential problem.

For low-Z braking, the upfiring Z jets are inhibited and braking comes from firing four X jets (two forward and two aft) simultaneously. Because of canting and scarfing effects, these X-jet thrust vectors are tilted 8 to 10° up from the +X-axes of the Orbiter. This gives a total thrust in the Z direction of about 260 pounds of force, resulting in an acceleration of 0.04 fps^2 for a 200 000-pound Orbiter. This is the least efficient braking technique in terms of propellant consumption, but it is needed for payloads that have little control authority and would lose attitude control if subjected to much plume impingement.

2.2.4 Sun and Roll Angles

The Sun angle (β angle) is the angle between the orbital plane and the sunline (from Sun to the center of Earth). For this mission, the Sun angle can range from $\beta = 0^\circ$ (Sun in the orbital plane) to a maximum of $\beta = 52^\circ$ (inclination of 28.5° , plus 23.5° angle between the ecliptic and equatorial planes).

Figure 3 shows the SMM and its body axes, and figure 4 shows the relationship of the control axes to the body axes. SMM points its +X-axis at the Sun, and since the SMM has limited control (ref. 1), it is free to rotate about the solar vector (+X-axis). The roll angle refers to the rotation about the X-axis which, practically speaking, will not be known but is useful in establishing flyaround procedures.

2.2.5 Onorbit Digital Autopilot

The onorbit DAP commands the Orbiter RCS jet firing activity during the onorbit flight phase. In the manual DAP mode, the system is driven with rotational and translational hand controller inputs. The THC has two modes of operation: acceleration and pulse. In the automatic DAP mode, several submodes are available, including a tracking mode and an Orbiter attitude-hold option. In the analyses both the manual and automatic capabilities of the DAP are used.

2.2.6 Universal Pointing Processor

The UPP can be used to supply inputs to the onorbit DAP to perform three basic pointing maneuvers. The three available options are LVLH hold, rotation, and maneuver. Under the LVLH option, the software will command a maneuver to point a vector fixed in Orbiter body axes at the center of the Earth. Under the rotation option, the Orbiter is rotated at a constant rate about a vector fixed in Orbiter body axes and in inertial space. Under the maneuver option the Orbiter maneuvers to a specified attitude. In these analyses all three options were used.

2.3 CANDIDATE FINAL APPROACH PROFILES

The various types of profiles can be divided into two categories: in-plane and out-of-plane profiles. These two types differ only in how the GF of a payload is visually acquired when the Orbiter is about 200 feet from the SMM. To fly an in-plane profile, the Orbiter stays in the orbital plane and "waits" for the SMM to rotate until the GF is in view. For an out-of-plane profile, the Orbiter flies out of the orbital plane and "finds" the GF.

Figure 5 shows five in-plane candidate profiles in a target-centered (SMM) LVLH coordinate system. Since the LVLH system rotates at orb rate, inertial approaches (which would appear as straight lines in an inertial frame) appear as curved lines. These profiles are discussed in more detail in section 3.3.1.

Figure 6 shows the basic out-of-plane candidate profile as seen in the X-Y plane of the target-centered LVLH frame. A zero beta angle is used in order to simplify the drawing. (For nonzero beta, the view in figure 6 would be of the plane perpendicular to the Sun line). The simulated profiles differ in whether they are performed in one or two phases, which depends upon how much is initially known about the SMM roll attitude. (The details will be discussed in section 3.3.2.) Some work was done on R-bar/out-of-plane approaches, and although they are straightforward for small beta angles, they are difficult for large beta angles. V-bar/out-of-plane approaches are preferred because they are not as dependent on the beta angle as the R-bar/out-of-plane approaches.

3.0 DISCUSSION

This section contains a detailed description of the SMM retrieval study, and several unique problems specific to SMM will be discussed. A complete explanation is also given of the profiles that were simulated and how the various problems are managed, as well as a description of the tools and techniques used in designing the profiles.

3.1 POTENTIAL PROBLEMS

The SMM shown in figure 3 is an inertially stable payload; the octagonal face of the SMM is kept pointed at the Sun. Several of the major factors considered in the profile design are discussed below. The factors can be thought of as potential problems because they add additional constraints to the proximity operations profiles.

Since SMM is only rate-damped about its X-axis, some type of maneuver to align the Orbiter and SMM (with GF visible and in a favorable position) must be incorporated into the profile. This maneuver must be independent of the SMM roll angle.

The SMM has 14.8 pounds-foot-seconds (ref. 1) of attitude control authority in each of two axes. This torque impulse comes from reaction wheels and is used to null external disturbances. Because of its large solar panels, the SMM is extremely sensitive to RCS plume impingement. This combination of plume

sensitivity and little control authority makes it very easy to tumble the SMM (e.g., an unbalanced force of 1 pound on one of the solar panels would cause loss of control in a few seconds). A tumbled SMM would not be recoverable in any reasonable timeline. Therefore, the plume impingement disturbances from these profiles must be negligible (smaller than gravity gradient effects) to avoid tumbling the SMM. A related concern involves remote manipulator system (RMS) loads and stresses caused by Orbiter PRCS jet activity; however, this problem is beyond the scope of this paper.

The GF is masked by one of the solar panels, with about eighteen inches clearance (ref. 2) between the GF and the panel. Because of the complex RMS configuration and the difficulty of maneuvering the arm in close quarters, several attempts have been made to arrive at a "best" SMM/Orbiter relative orientation for grappling. This configuration, with the X-axes aligned and the GF in the COAS view, is shown in figure 7 (from ref. 3). Upon completion of the final approach profile, the two vehicles should be properly aligned and ready for the grappling operation.

Since the techniques proposed in this document involve out-of-plane flyarounds, the effects of orbital mechanics on the performance of the maneuver must be considered. For example, if the Orbiter leaves the target orbital plane and flies out along the angular momentum vector, the two orbital planes will cross 180° of orbit travel later. This would result in increased propellant consumption if the Orbiter moved farther out along the angular momentum vector. Out-of-plane maneuvers could become very difficult and expensive if performed manually. The approach of this study has been to use the DAP and UPP features whenever they would reduce the pilot workload, improve efficiency, or make the maneuver easier.

These profiles should be independent of the beta angle. According to the September 1979 Flight Manifest (ref. 4), the inclination angle will be 28.5° . Prior to launch, the beta angle will be known; however, at this time it is known only that the beta angle will be less than 52° .

Other factors to consider are pilot workload and propellant consumption. Since Orbiter PRCS propellant is limited, especially in the forward tank, one goal is to minimize propellant consumption and still accomplish the mission. Also, the profile must be realistic in terms of the demands made of the pilot(s), mission specialist, and RMS operator.

3.2 METHODOLOGY

The tools and techniques used to perform the SMM retrieval study are discussed in the next few paragraphs. Basic analysis assumptions are shown in table I.

Although the September 1979 Flight Manifest indicates that the inclination will be 28.5° , several other angles were used as well. Also, the simulations were run for various beta angles. All simulations begin at a range of 1000 feet and end at a range of 30 to 40 feet. Since the SMM Sun roll angle is variable (and may not be known premission) it is assumed that the GF orientation is unknown; the SMM roll rate is assumed negligible.

The basic tool is the proximity operations/plume impingement simulation (POPIS) that integrates the plume impingement and paper-pilot models with the space vehicle dynamics simulation (SVDS) program (ref. 5). This tool gives a two-vehicle, 12-degree-of-freedom digital simulation of onorbit proximity operations. For a detailed explanation of the tools and capabilities, see reference 6. The primary purpose of these simulations is to generate payload disturbance data (forces and torques) and Orbiter PRCS propellant consumption data, which are used in assessing the feasibility of the proximity operations segment of the mission.

The geometry models used for SMM, shown in figure 8, can be compared with the actual SMM of figure 3. The simpler model in figure 8 is used for complete simulations in POPIS.

The basic logic for the paper-pilot models is shown in figure 9. This logic is used for all approach types (R-bar, V-bar, inertial) discussed earlier. The cross-axis logic will keep the payload centered in the COAS field of view, while the approach-axis logic will keep the Orbiter moving away from or towards the payload at the desired rate. The desired rates are input by the user, as are the limits of the COAS field of view and the frequencies at which each type of logic is executed.

3.3 FINAL APPROACH PROFILES

3.3.1 In-Plane Profile

The first phase of an in-plane profile is to approach from 1000 feet with the Orbiter in LVLH hold, stopping at a range of about 200 feet from the payload. If the GF is in sight and the SMM is favorably oriented with respect to the Orbiter, the pilot would place the Orbiter in an inertial-hold mode and continue the approach along the line-of-sight vector to the GF. Thus, the final 200 feet would be flown as an inertial approach in the X-Z LVLH plane (profile 2 of fig. 4).

If upon reaching 200 feet, the GF is not in sight or if the SMM/Orbiter alignment is not correct for grappling, it may be possible for the Orbiter to stationkeep and wait until conditions are favorable for beginning the final approach. This technique can work because the Orbiter is in LVLH hold and the SMM is in an inertial hold, rotating relative to the LVLH frame. If the Orbiter could stationkeep and wait long enough (given the time and propellant constraints), the GF may rotate around and come into view. At this point, the pilot would switch to inertial hold and continue the approach along the line-of-sight vector to the payload. The problem with this method is that it is difficult to know how long it will take for the GF to come into view; indeed, for some orientations it will never come into view.

If the GF is in the orbital plane (or close to it) the pilot could switch DAP modes and initiate a pitch maneuver to fly around the SMM in the orbital plane until the GF is visible (fig. 10). This, however, assumes knowledge of the Sun-roll angle, over which there is little control and possibly no information.

Besides, if the GF is too far out of the orbital plane this technique would not work.

The in-plane techniques depend on chance and cannot be relied on to give a clear view of the GF because of the lack of control and information about the roll angle of the SMM. (Having sight of the GF is not a guarantee that the SMM will be recoverable, but it is a necessary first step.) While in-plane techniques are not completely satisfactory, the following methods result in a clear view of the GF and proper alinement before moving from 200 to 30 feet.

3.3.2 Out-of-Plane Profile

The initial and final phases of the approach profile are identical to the in-plane techniques. That is, the V-bar approach is started at 1000 feet and stops at 200 feet; when the two vehicles are properly alined (GF in sight), the Orbiter DAP is switched into inertial hold and the approach continues along the line-of-sight vector, stopping at 30 feet. The differences are in the methods used to aline the two vehicles and visually acquire the GF. The technique proposed in this document is shown in figure 11.

The first step occurs at 200 feet and consists of alining the +X-axes of the Orbiter and SMM so that they are parallel. Since the beta angle will be known at the time of the flight, this maneuver can be done automatically. The DAP/UPP inputs can be either precomputed and stored or uplinked in real time so that they will be available when needed. Since the maneuver rate is also a DAP/UPP input, the time it will take to execute the maneuver will vary. The maneuver has been simulated at 0.2 to 0.4 deg/sec, and it takes 2 to 3 minutes to aline the X-axes of the two vehicles for a maximum beta of 52° . Alining is basically a yaw-pitch maneuver for the Orbiter; during this operation the pilot keeps the SMM centered in the COAS via THC deflections (also simulated).

After the +X-axes are alined, the pilot initiates the second step by commanding a constant rate (0.2 to 0.4 deg/sec) rotation maneuver about the Orbiter X-axis. (Whether a positive or negative roll is required is determined prior to the maneuver.) Once again, this is an automatic maneuver which requires that the pilot switch DAP modes. The direction of the Orbiter X-axis will be held fixed in inertial space, keeping the SMM and Orbiter +X-axes parallel. As the Orbiter rolls, the payload will tend to move out of the COAS field-of-view; the pilot will command Y-axis translations to keep SMM centered in the COAS. The net result is an out-of-plane flyaround (fig. 12).

At most, the pilot should have to fly around 180° to bring the GF into the desired position, which means that this could take as long as 15 minutes. The alinement/flyaround phase could thus take as long as 18 minutes. As before, the pilot would then switch to inertial hold and complete his approach.

If the SMM roll angle is known the proper DAP/UPP inputs can be made and the two-phase method described earlier can be accomplished in one phase in no more than 15 minutes. The +X-axes are not necessarily alined at the start but the pilot commands a constant rate rotation that terminates with the GF in sight and the vehicles alined (fig. 13) before initiating the final approach.

3.4 COMPARISONS

The major advantage of out-of-plane flyaround techniques over the in-plane techniques is that they work for any beta or for any Sun-roll angle. Since there is no extended stationkeeping in the out-of-plane techniques, there could be a propellant savings over the in-plane methods. Both techniques are semiautomatic maneuvers (automatic attitude control and manual translation). The maneuver rates and times are variable for all the techniques. The major disadvantage of the in-plane techniques is that there is no guarantee that the GF will ever come into view or be oriented favorably for grappling without some out-of-plane maneuvering. Both rely on optical ranging and both are performed at ranges of 200 feet \pm 20 feet. All of the techniques have been simulated on digital computers; however, none have been analyzed in man-in-loop simulations.

4.0 SIMULATION RESULTS

The results are divided into two parts: inplane and out of plane. Generally speaking, the 0.2 to 0.4 deg/sec maneuver rate is acceptable for all techniques, and the plume impingement disturbances are acceptable if the low-Z braking mode is used. The simulation times given do not include actual grappling or any time between phases (such as stationkeeping while waiting for the GF to rotate into view).

4.1 IN-PLANE RESULTS

Table II contains propellant and impingement data. Note that only low-Z braking results in acceptable impingement disturbances (including gravity-gradient torques) and that both R-bar and V-bar approaches are feasible in the low-Z mode. Stationkeeping on V-bar uses less propellant than on R-bar, since less cross-axis jet activity is required to keep the payload centered in the COAS, again because of orbital mechanics. However, since there is no "natural braking" on V-bar, all the delta-V used to approach the payload must be taken out by firing jets in the direction of the SMM (either +Z or +X). The +X jets provide about one-fifth as much braking as the +Z jets so the +X jets must be fired five times as long to null out the same amount of delta-V, thus increasing propellant requirements for the low-Z approaches. The inertial flyaround maneuvers require about the same amount of propellant regardless of whether they are initiated on R-bar or V-bar. The complete R-bar profiles use about the same amount of propellant as the complete V-bar profiles. Because V-bar approaches are easier for pilots to fly, the V-bar profiles are preferred.

Inertial approaches from 1000 feet are slightly more expensive, more difficult, and not necessary. Switching to an inertial approach at 200 feet does not pose a problem (in these simulations) but is a little more difficult than a pure V-bar profile.

Finally, it is important to note that for certain beta/Sun-roll combinations the in-plane approaches may not result in favorable conditions for grappling.

4.2 OUT-OF-PLANE RESULTS

Since V-bar approaches are preferred from a flight operations point of view the out-of-plane simulations were initiated on V-bar. Table III contains the results of the one-phase and two-phase flyaround techniques. Although the one-phase flyaround uses less propellant and less time, it relies upon having data about the SMM orientation prior to the maneuver; if the data were wrong, the GF might not be favorably oriented at the end of the operation. The simulations indicate that the two-phase flyaround will work even with no knowledge of the SMM roll angle. It will also work for any beta angle. This method is general enough to be used for retrieving all inertially stabilized payloads.

4.3 SIMULATION PLOTS

The data in figures 14 to 16 are from the same in-plane approach profile, consisting of a V-bar approach from 1000 feet to 200 feet followed by an inertial approach from 200 feet to grapple range. Figures 17 to 20 present similar data for an out-of-plane profile: a V-bar approach from 1000 feet to 200 feet, a two-phase flyaround, and finally an inertial approach from 200 feet to 30 feet. Both profiles used the low-Z braking mode.

Figures 14 and 17 are plots of range versus closing rate of the Orbiter relative to the target. In figure 14 the braking gates are clear at 600 feet, 300 feet and 35 feet. In figure 17 the activity at 200 feet indicates that the Orbiter is no longer approaching the SMM (this is where the flyaround occurs).

A torque history chart shows the cumulative torque impulse on the SMM is due to plume impingement, and gravity gradient effects. The "smooth" contours of figure 15 indicate that most of the torque is due to gravity gradient effects, whereas the "steps" in figure 18 correspond to plume disturbances caused by Orbiter braking.

Figures 16 and 19 give the time history of the propellant usage for each profile. The sudden vertical rises correspond to braking maneuvers. The high propellant consumption is due to +X braking. By looking at figure 19 and knowing that the flyaround occurred from 18 to 36 minutes into the simulation, it can be determined that 700 pounds of propellant are used for the flyaround. "FWD" and "AFT" refer to the forward and aft RCS tanks.

Figure 20 gives a "third-person" view looking down on the X-Y LVLH plane and clearly shows the out-of-plane flyaround.

5.0 CONCLUSIONS

This study has demonstrated that SMM retrieval is feasible in terms of plume disturbances, propellant consumption, time, and pilot workload. Both R-bar and V-bar approach profiles are acceptable; however, V-bar is preferred. It was found that the profile must be flown in the low-Z mode so that the SMM will not be tumbled.

6.0 RECOMMENDATIONS

As a result of the analyses performed, the following profile is recommended: a V-bar approach from 1000 feet to 200 feet, a two-phase flyaround to visually acquire the grapple fixture and orient the two vehicles, and then an inertial approach from 200 feet to 30 feet.

Although the simulation data indicate that these techniques will work, man-in-loop simulation data are still needed. There may be problems integrating an onorbit DAP into the real-time simulator, but it is advisable that these simulations, especially the flyarounds, be made.

Finally, it is recommended that studies be initiated to look at potential problems involving maneuvering the Orbiter with an unstowed RMS. The maximum translational rates achieved are as high as 0.7 fps for the proposed maneuvers, and it is necessary to know if the arm can tolerate the resulting loads.

7.0 REFERENCES

1. Pandelides, J.: SMM System Design Specification. 409-2004-0002, January 1979.
2. Bello, A. J.: SMM Conceptual Arrangement. GE 1089536, March 1978.
3. Mosel, D. K.: SMM Rendezvous/Proximity Operations Status. July 1979.
4. Flight Assignment Manifest. 13000-0-6T, September 1979.
5. Mission Planning and Analysis Division: Space Vehicle Dynamics Simulation (SVDS) Program. JSC-11157, October 1977.
6. Schoonmaker, P. B.: POPIS Overview Document. TM 1.4-MAB-310, April 1979.

TABLE I.- ANALYSIS ASSUMPTIONS

Parameter	Orbiter	SMH
Mass, lb	214 000	4939
Control system	Digital autopilot	Reaction wheels
Control system deadbands	1°, 0.2 deg/sec	Wheel saturation
Control	Auto attitude control manual translation	Auto attitude control
Altitude, n. mi.	275	No translation
Momentum storage lb-ft-sec (N-m-sec)	N/A	275
Attitude	Three-axis control	14.8 (20)/wheel
Inertias, slug-ft ²		Two-axis solar inertial hold; rate-damped Sun roll
IXX	790 900	1261
IYY	6 092 000	2639
IZZ	6 307 000	2713
IXY	-3 000	7.4
IXZ	-134 000	-156.3
IYZ	-1 000	-12.9

TABLE 1. N-PLANE SIMULATION RESULTS

Profile no., run no.	Profile	Orbite braking mode	Time, min	SMM rltume disturbance (abs. cum.) : X,Y,Z lb-ft-sec	Orbiter RCS propellant, lb-mass
1, 39	V-bar	Norm-Z	30	6, <u>a18</u> , <u>78</u>	315
1, 34		Low-Z	28	1, 4, 8	635
2, 38	V-bar/inertial	Norm-Z	35	8, 12, <u>69</u>	330
2, 35		Low-Z	28	3, 8	705
2, 48 ^{bc}		Low-Z	24	1, 1	520
4, 3	R-bar	Norm-Z	33	<u>20</u> , <u>65</u>	350
4, 18		Low-Z	29	2, 4	570
5, 17	R-bar/inertial	Norm-Z	37	7, <u>32</u>	350
5, 41 ^c		Low-Z	29	1, 2, 5	530
3, 27 ^c	Inertial	Low-Z	35	1, 1, 5	760

^aUnderlined numbers indicate that SMM control priority was exceeded.

^bRun 48 is the same as run 35 except a more efficient braking schedule and lower stationkeeping rates were used.

^cSame braking schedule and stationkeeping rates were used.

TABLE III.- OUT-OF-PLANE SIMULATION RESULTS

Run no.	Profile/flyaround type	Orbiter braking mode	Time, min	SMM plume disturbance (abs. cum.) : X,Y,Z lb-ft-sec	Orbiter RCS propellant, lb-mass
56	V-bar/2 phase (180°)	Low-Z	47	1,1,7	1389
58 ^a	V-bar/2 phase (180°)	Low-Z	45	1,1,6	1129
59	V-bar/2 phase (90°)	Low-Z	38	1,1,4	803
59	V-bar/1 phase (180°)	Low-Z	44	1,1,7	1601
63 ^b	V-bar/1 phase (180°)	Low-Z	45	1,1,7	1480

^aRun 58 is the same as run 56 except a more efficient braking schedule was used.

^bRun 63 is the same as run 59 except a more efficient braking schedule was used.

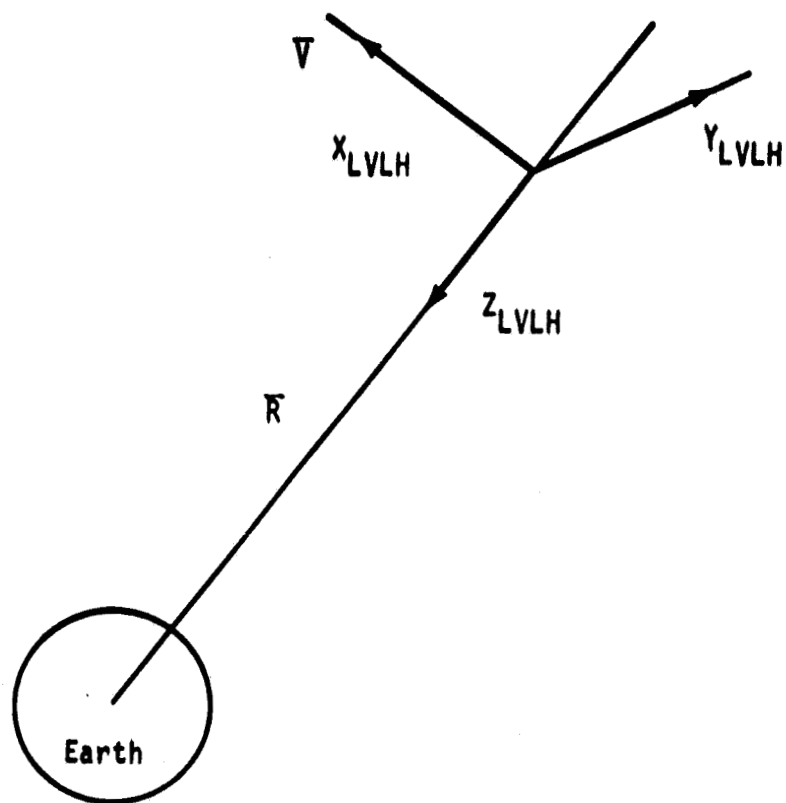


Figure 1.- Local vertical/local horizontal coordinate system.



Payload

Jet centerline

PRCS plumes

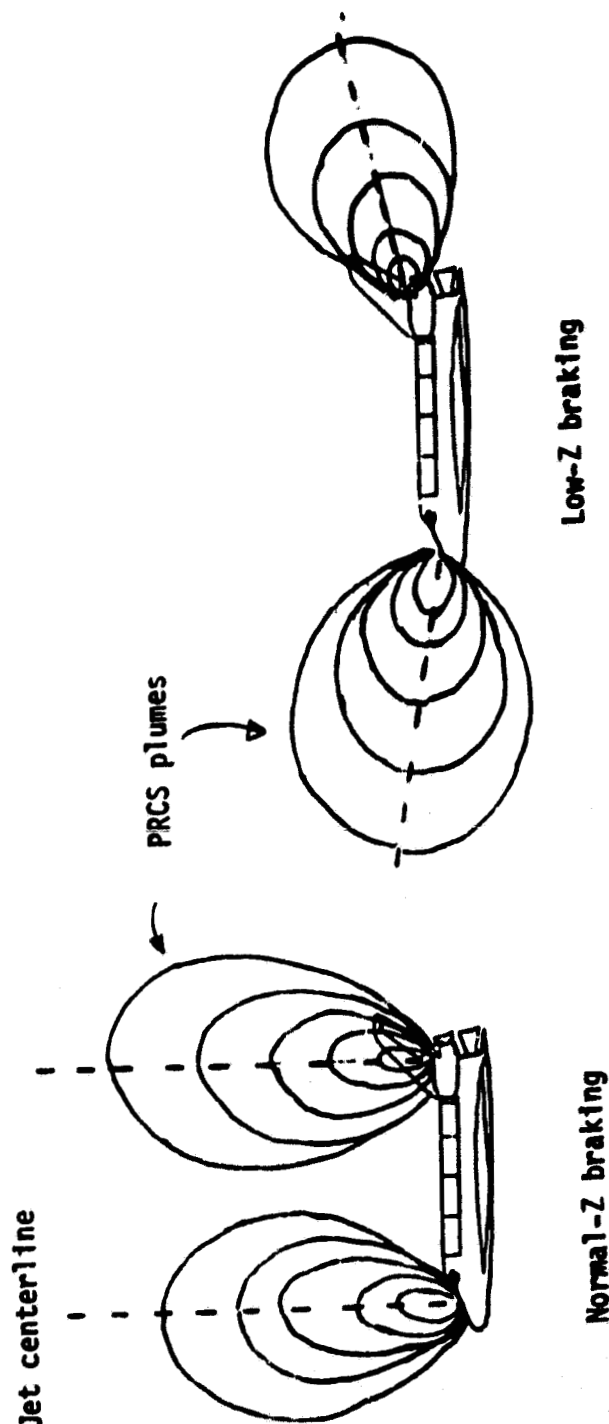


Figure 2.- Braking methods.

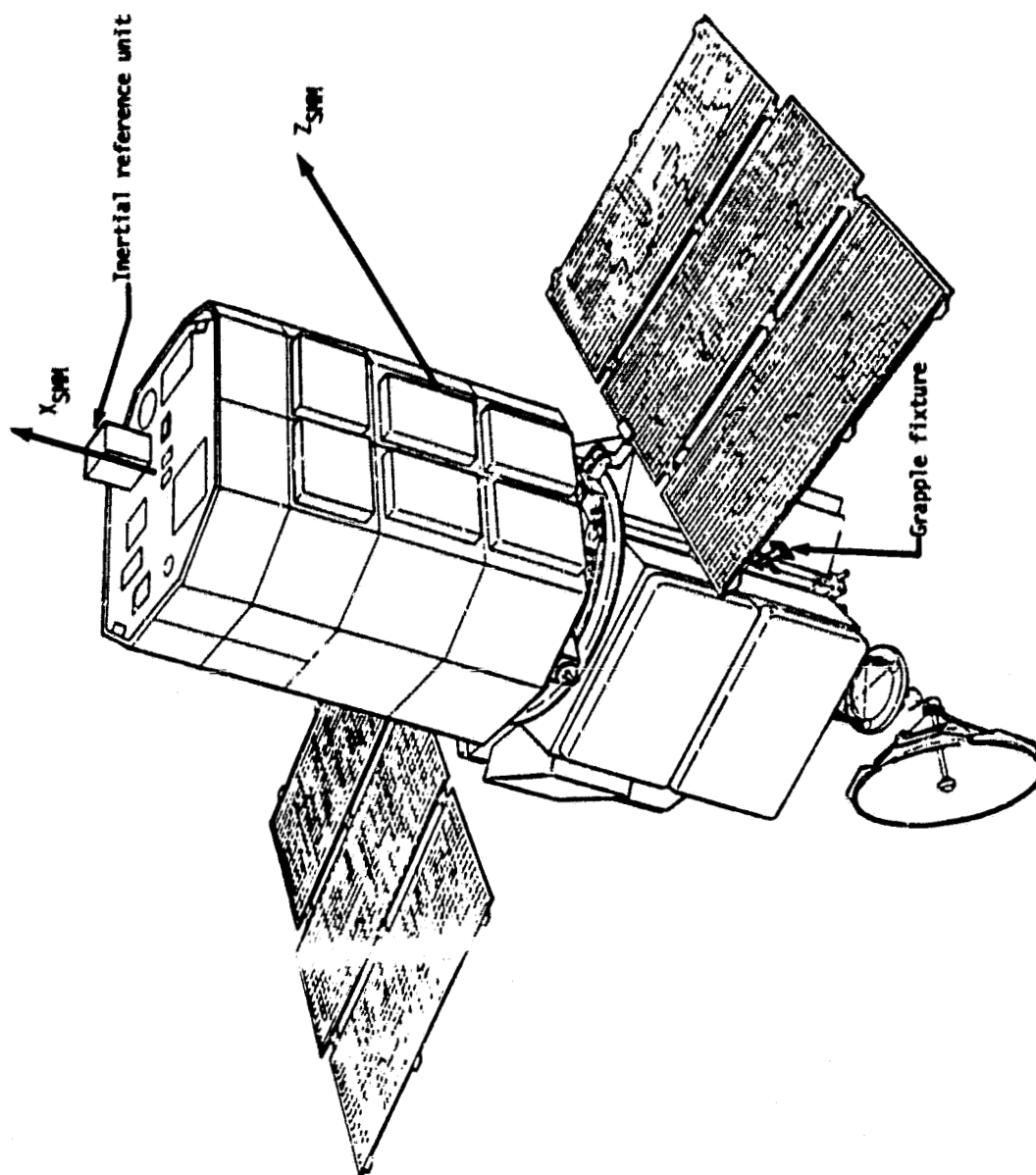


Figure 3.- Solar maximum mission observatory.

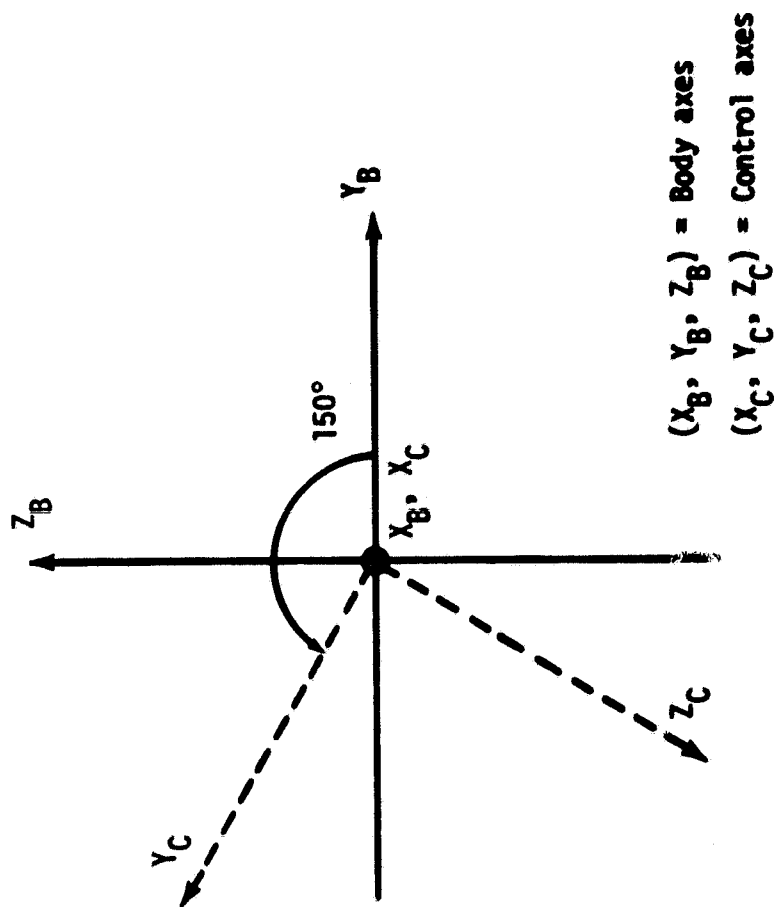


Figure 4.- SHM control axes.

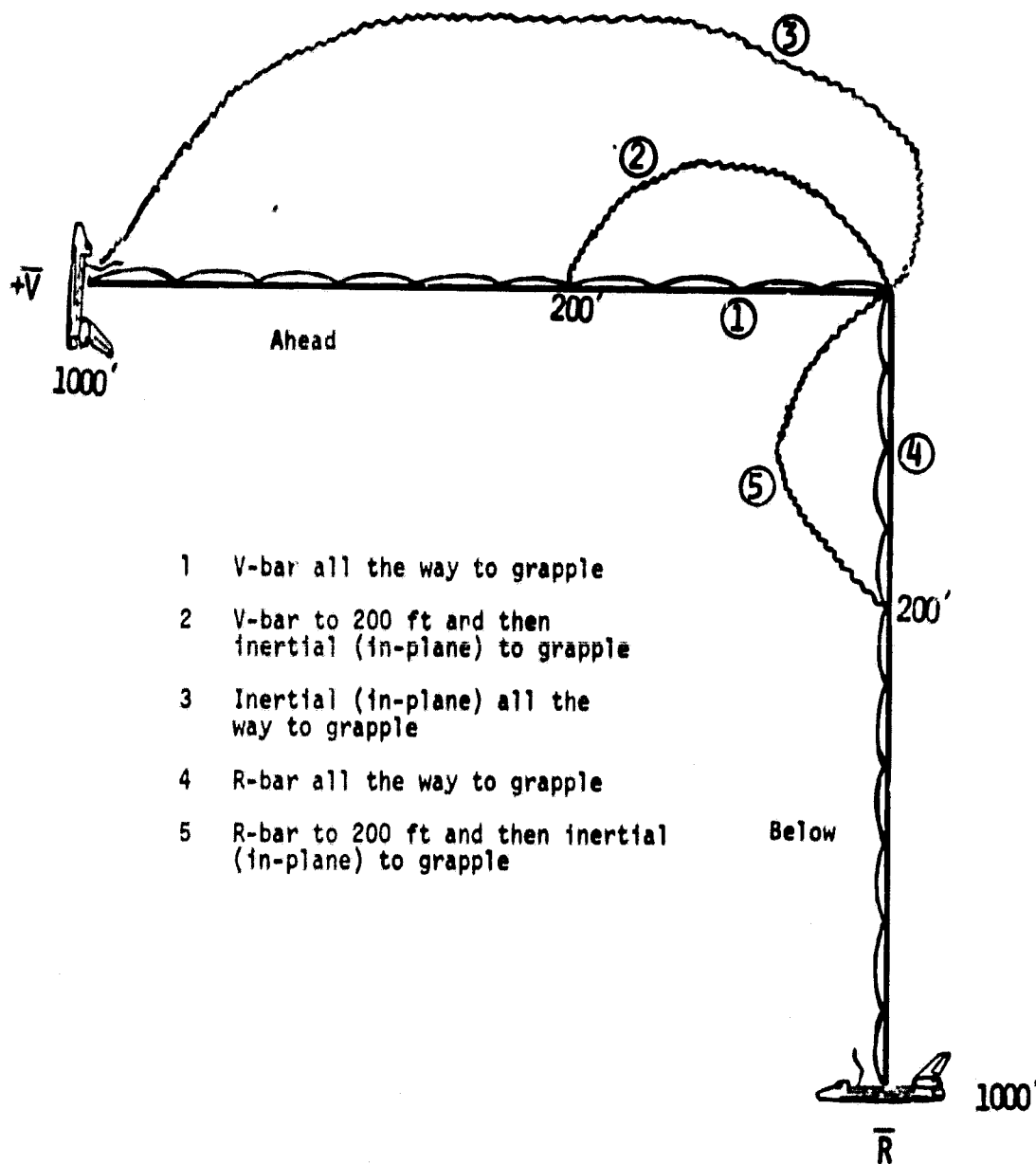


Figure 5.- In-plane approach profile.

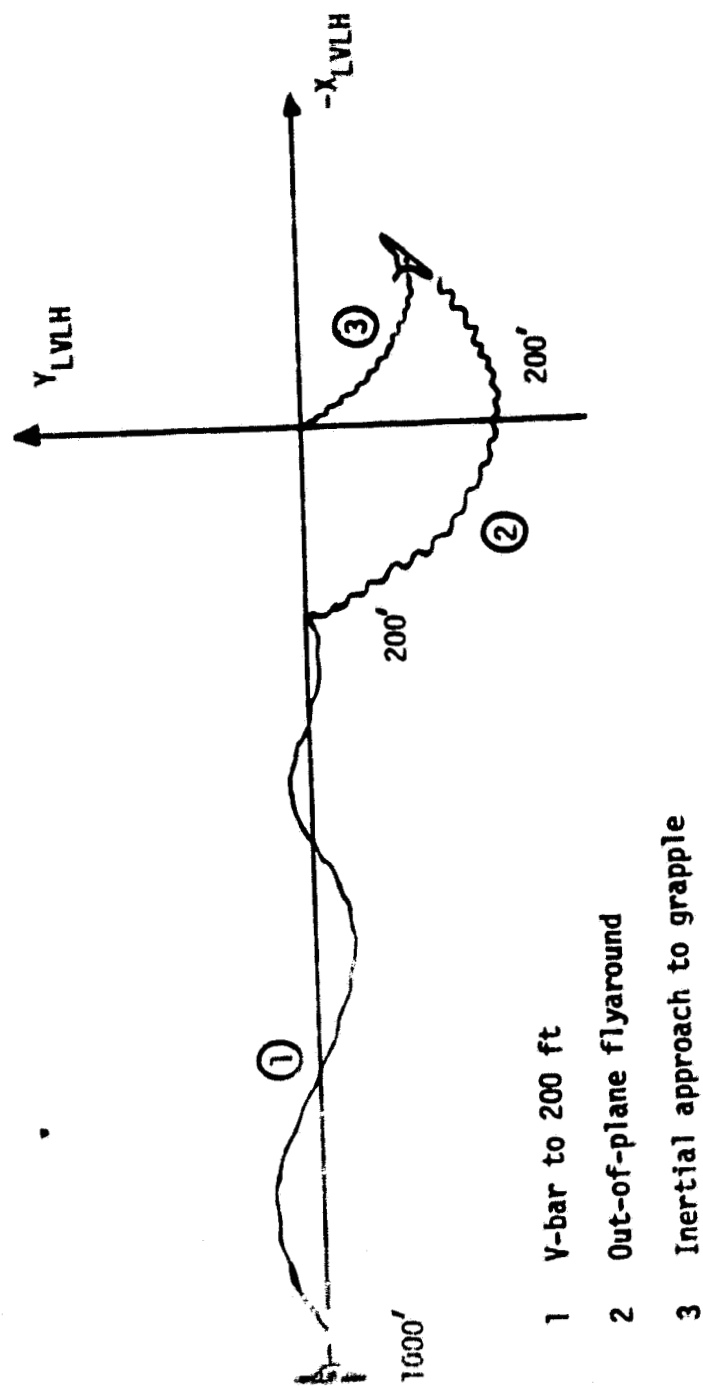


Figure 6.- Out-of-plane approach profile.

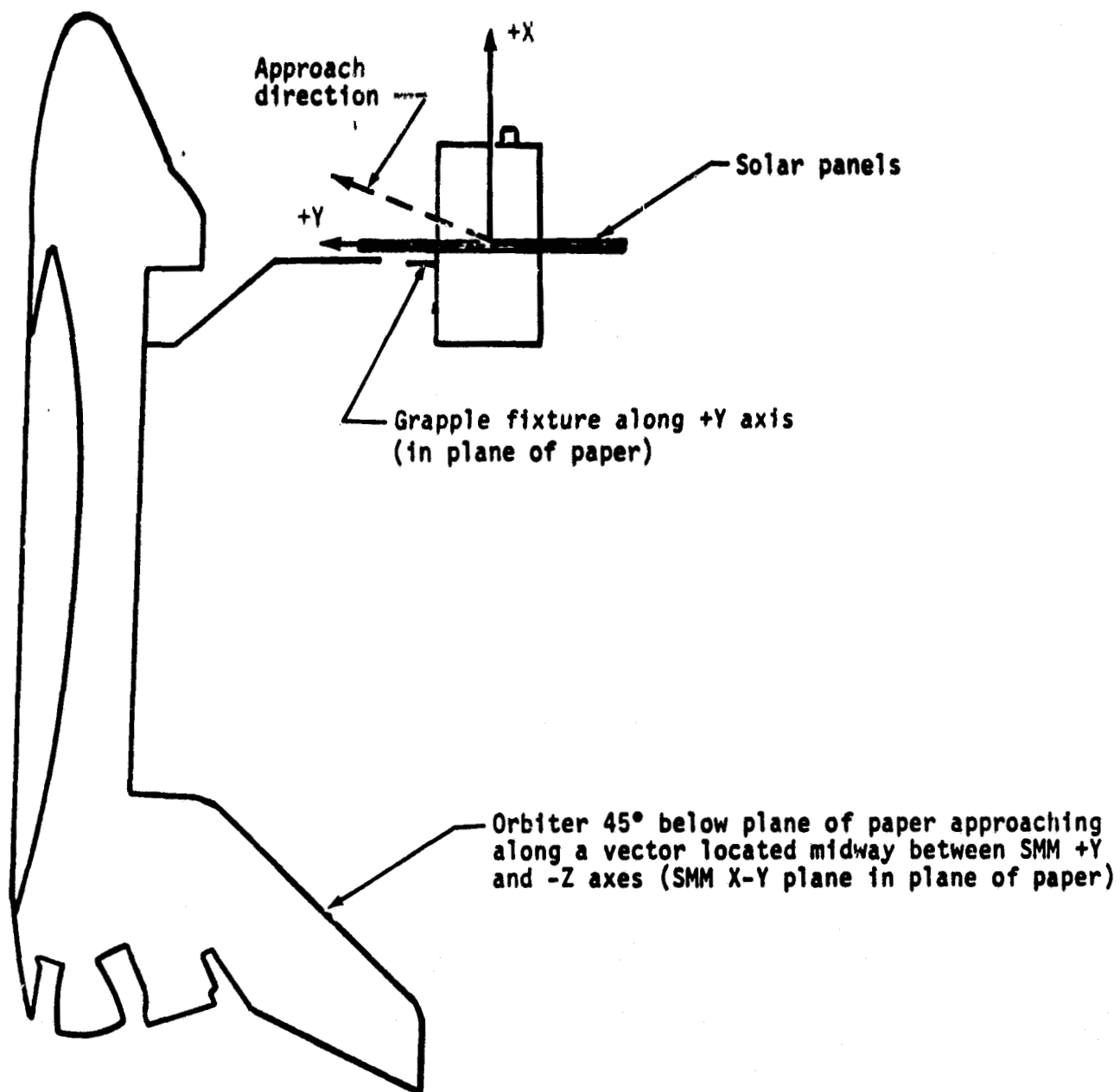


Figure 7.- Desired alignment prior to grapple.

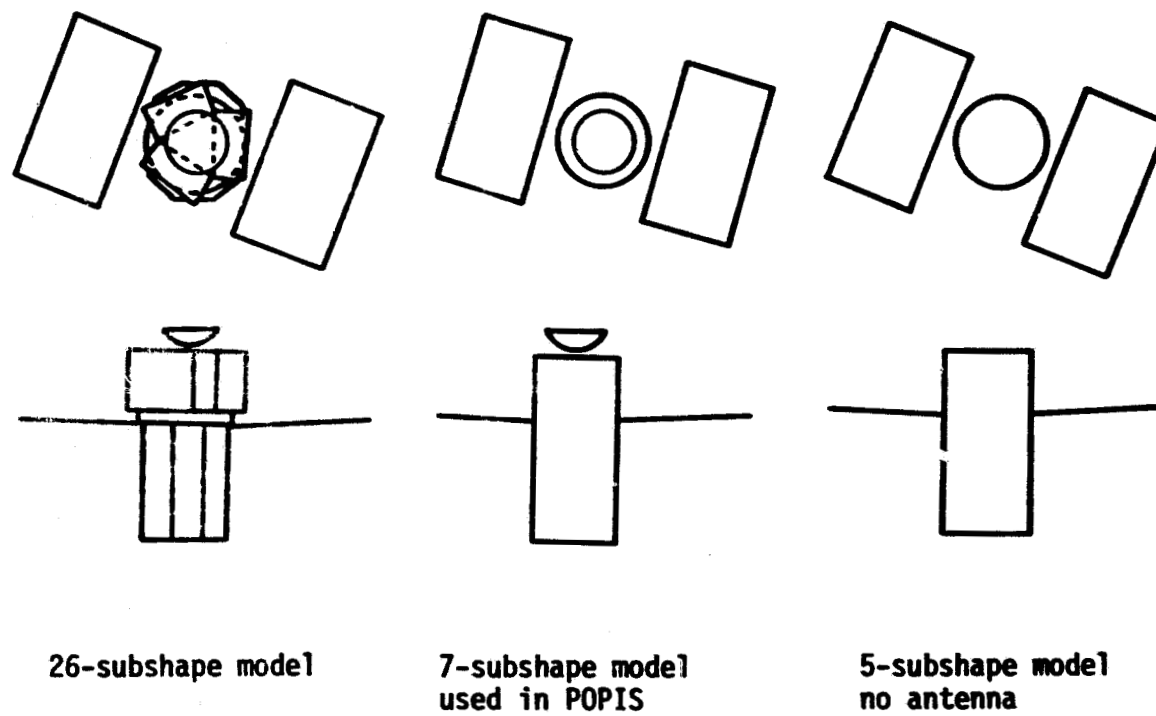


Figure 8.- Geometry models for SMM configuration.

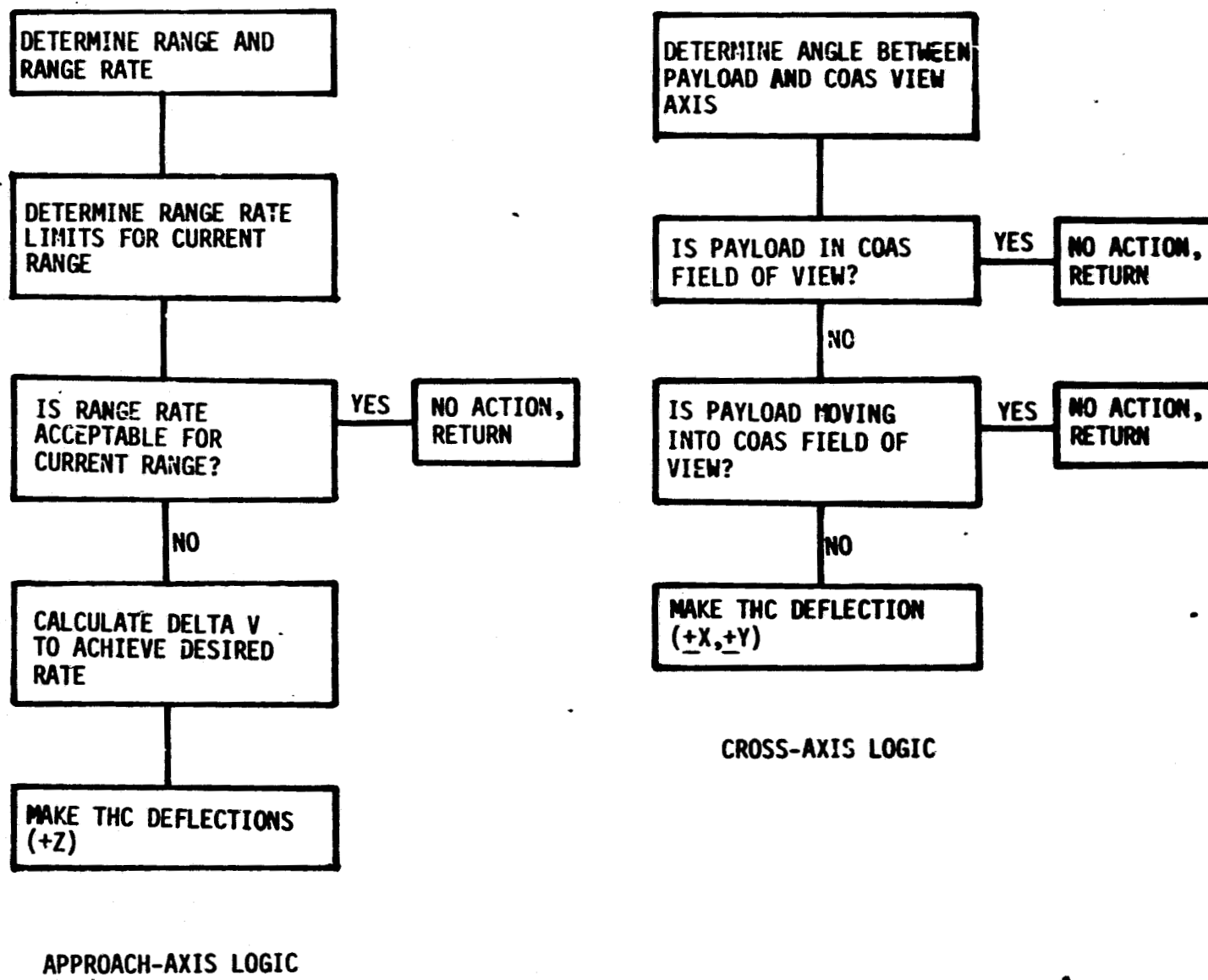
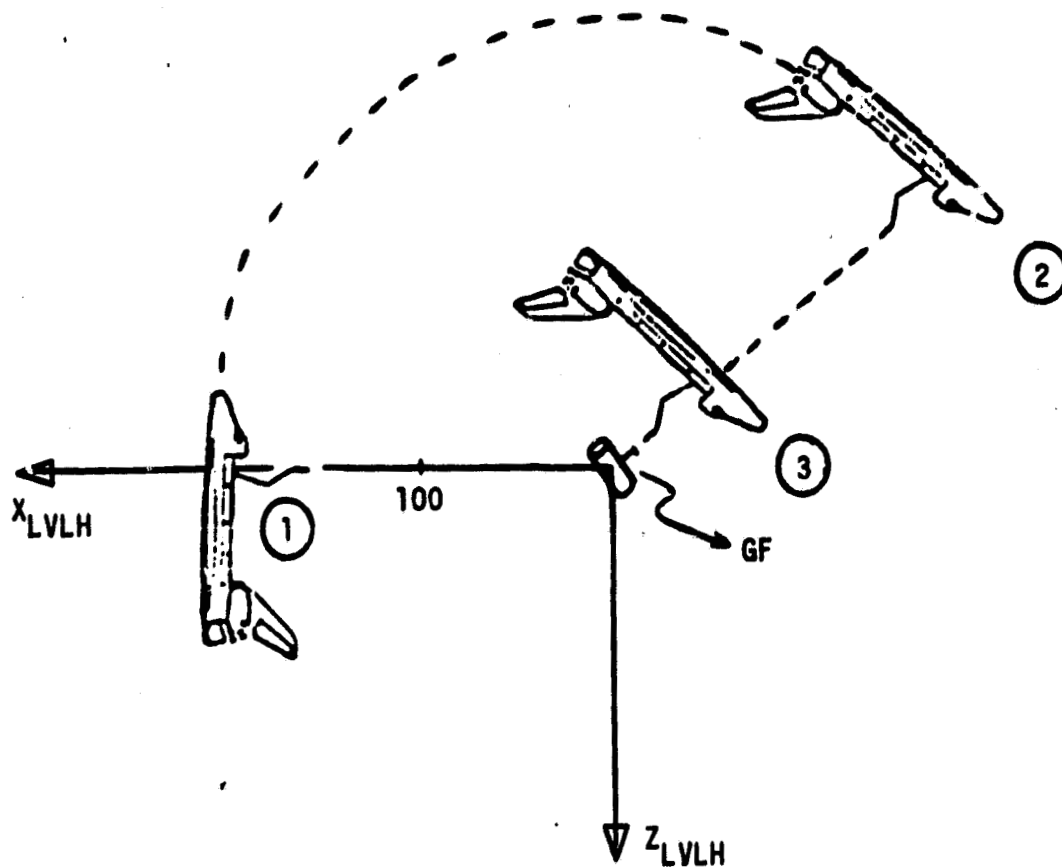
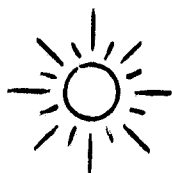
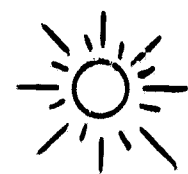


Figure 9.- Paper pilot logic.

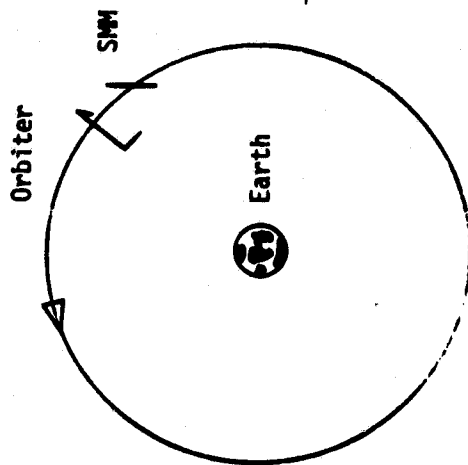


- ① At 200 ft begin pitch maneuver to initiate flyaround
- ② Visually acquire GF and align Orbiter and SMM
- ③ Approach along line-of-sight to 30 ft

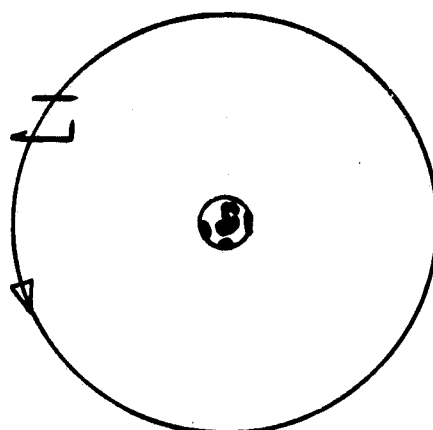
Figure 10.- Flyaround and final approach for GF in orbital plane.



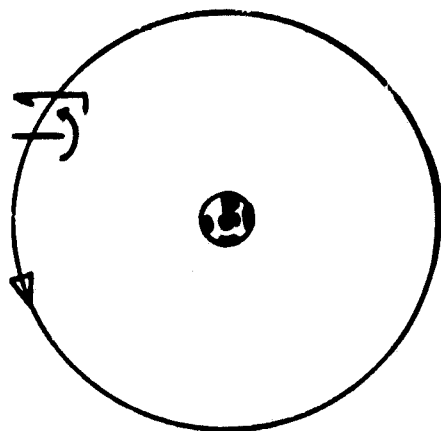
Sun



Orbiter in LVLH hold with -X axis pointed at center of Earth; SMM pointed at Sun.

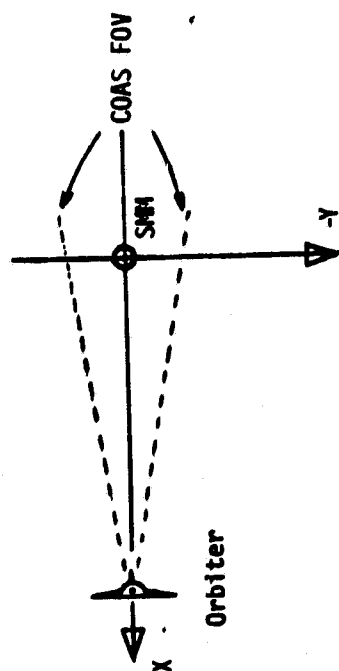


Phase 1 - Align +X-axis of Orbiter with +X-axis of SMM

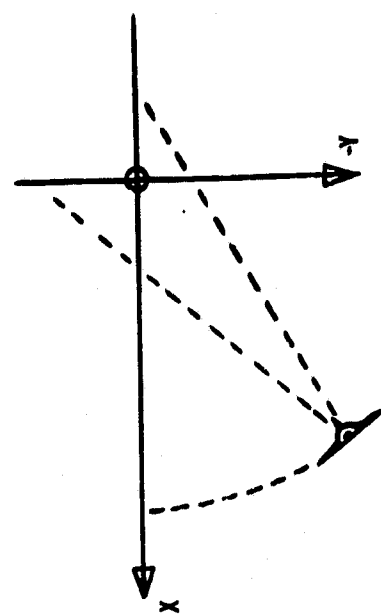


Phase 2 - Roll Orbiter and perform flyaround keeping Orbiter X-axis fixed in inertial space

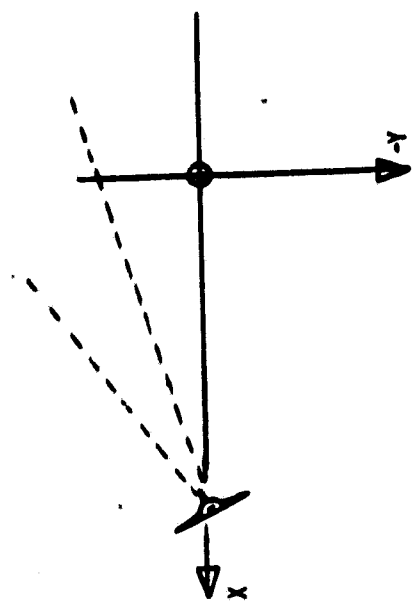
Figure 11.- Two-phase flyaround.



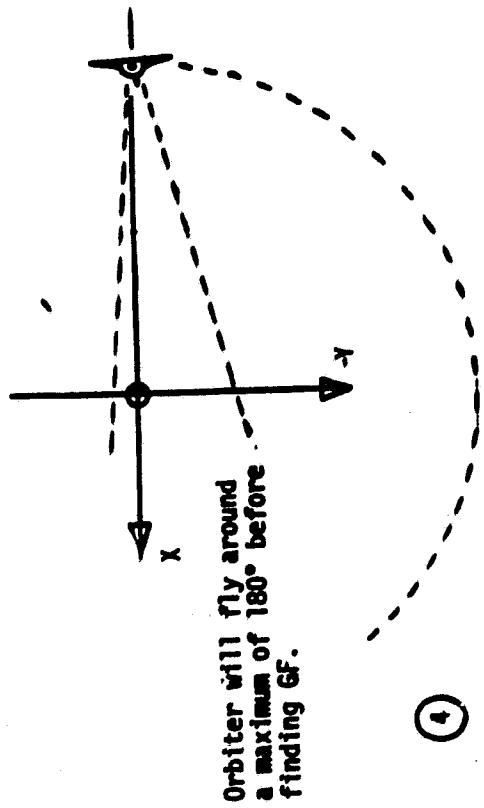
① Orbiter initiates automatic roll maneuver with SMH in COAS field-of-view.



③ Pilot manually translates to keep SMH in COAS field-of-view.



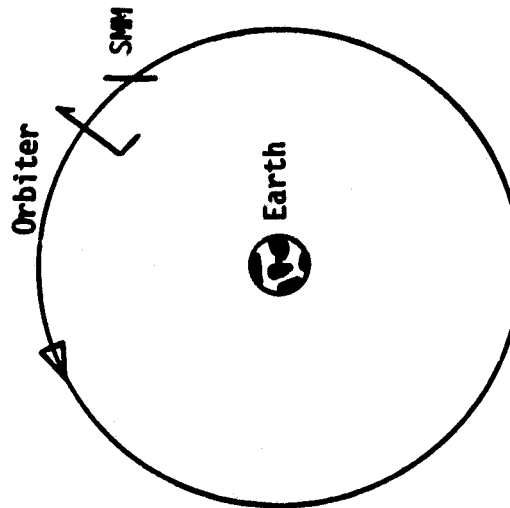
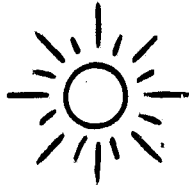
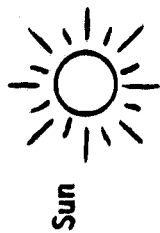
② As the Orbiter rolls the SMH moves toward the COAS field-of-view limits.



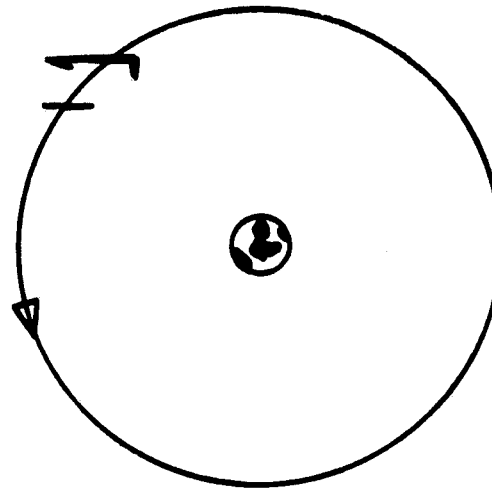
Orbiter will fly around a maximum of 180° before finding GF.

④

Figure 12.- Automatic roll and manually centering SMH in COAS results in flyaround.



Initialize on V-bar with
Orbiter in LVLH hold



Phase 1 - A single rotation will result in
aligning X axes and flying around

Figure 13.- One-phase flyaround.

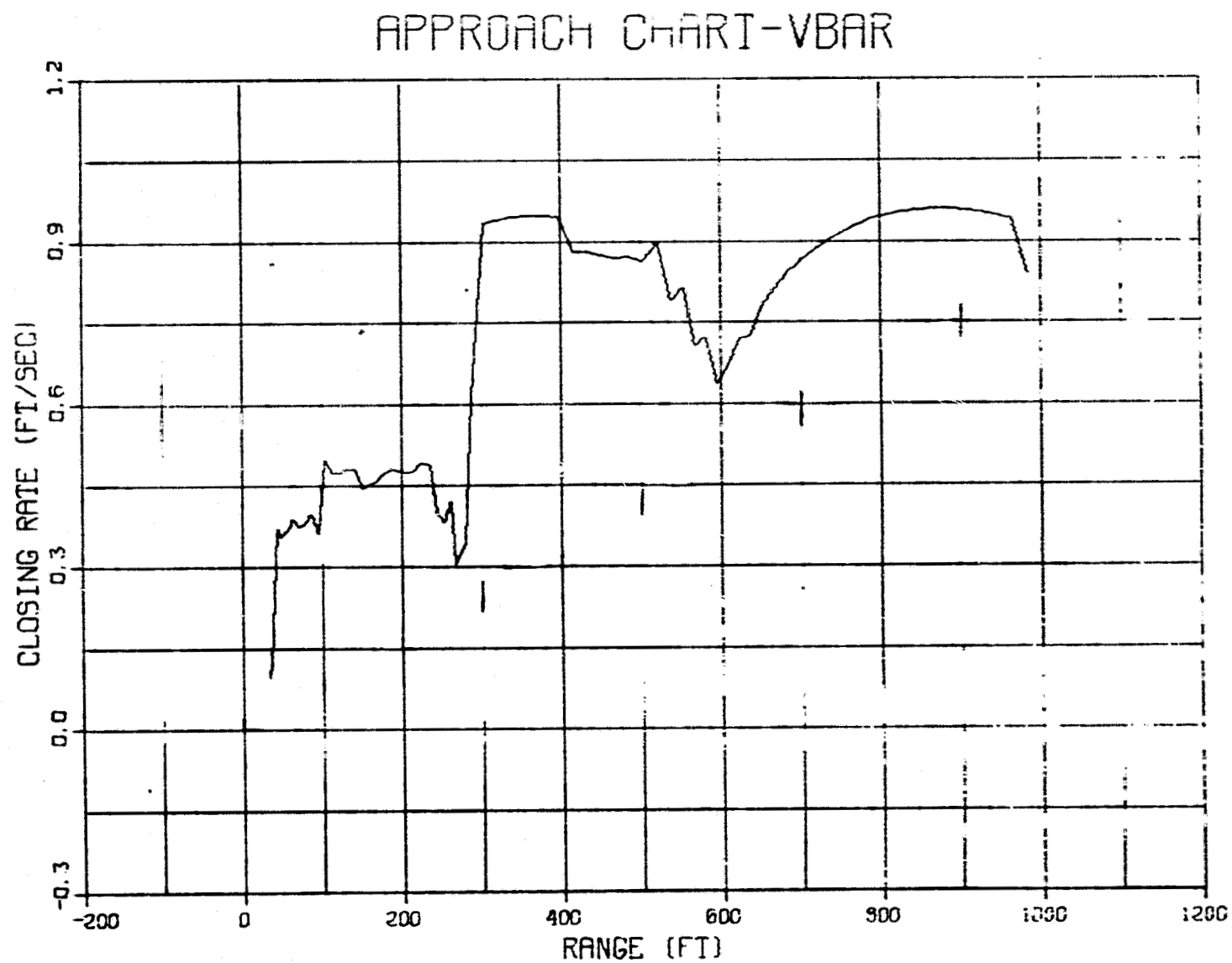


Figure 14.- Approach chart (in-plane profile).

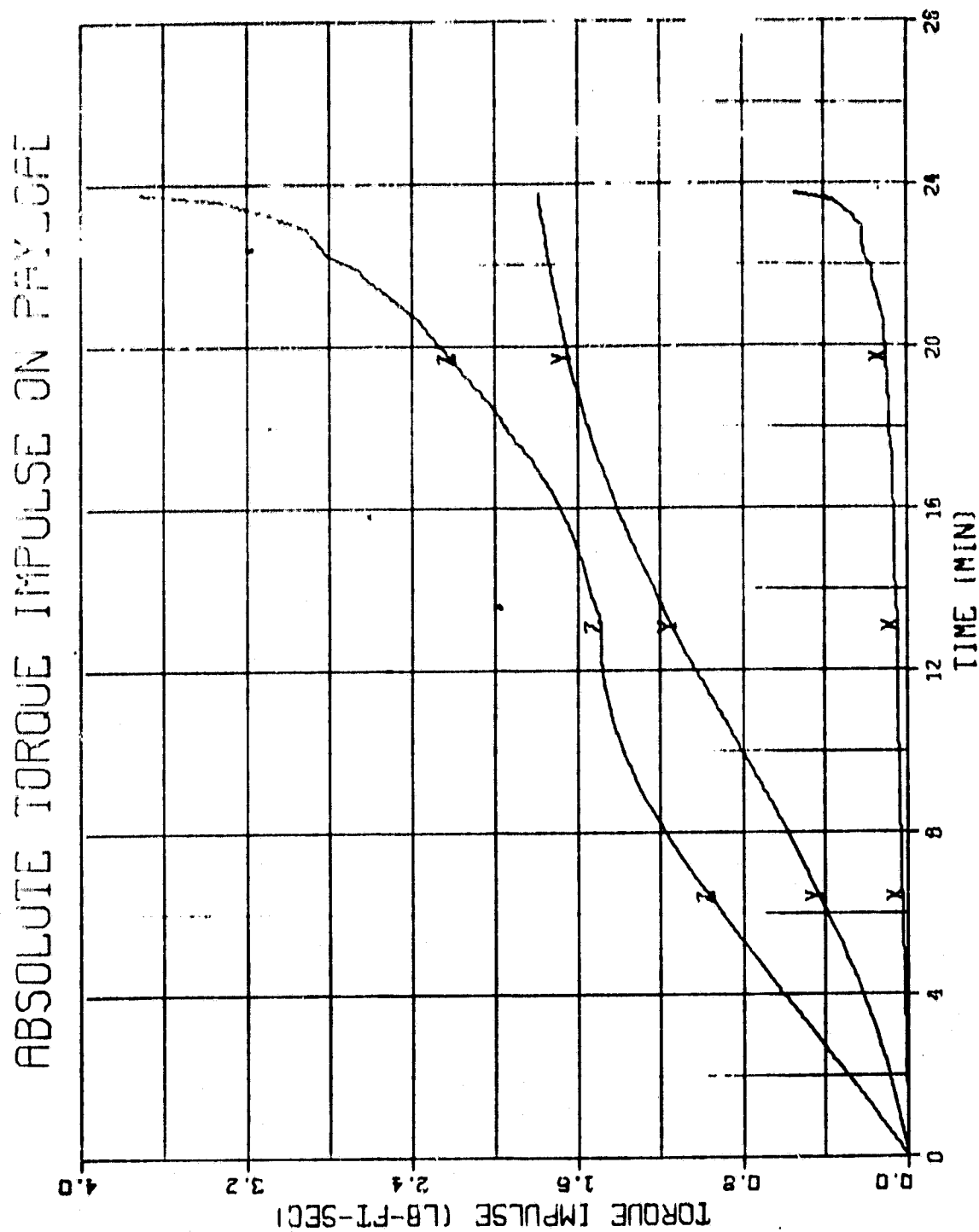


Figure 15.- Torque impulse history (in-plane profile).

PROPELLANT CONSUMPTION

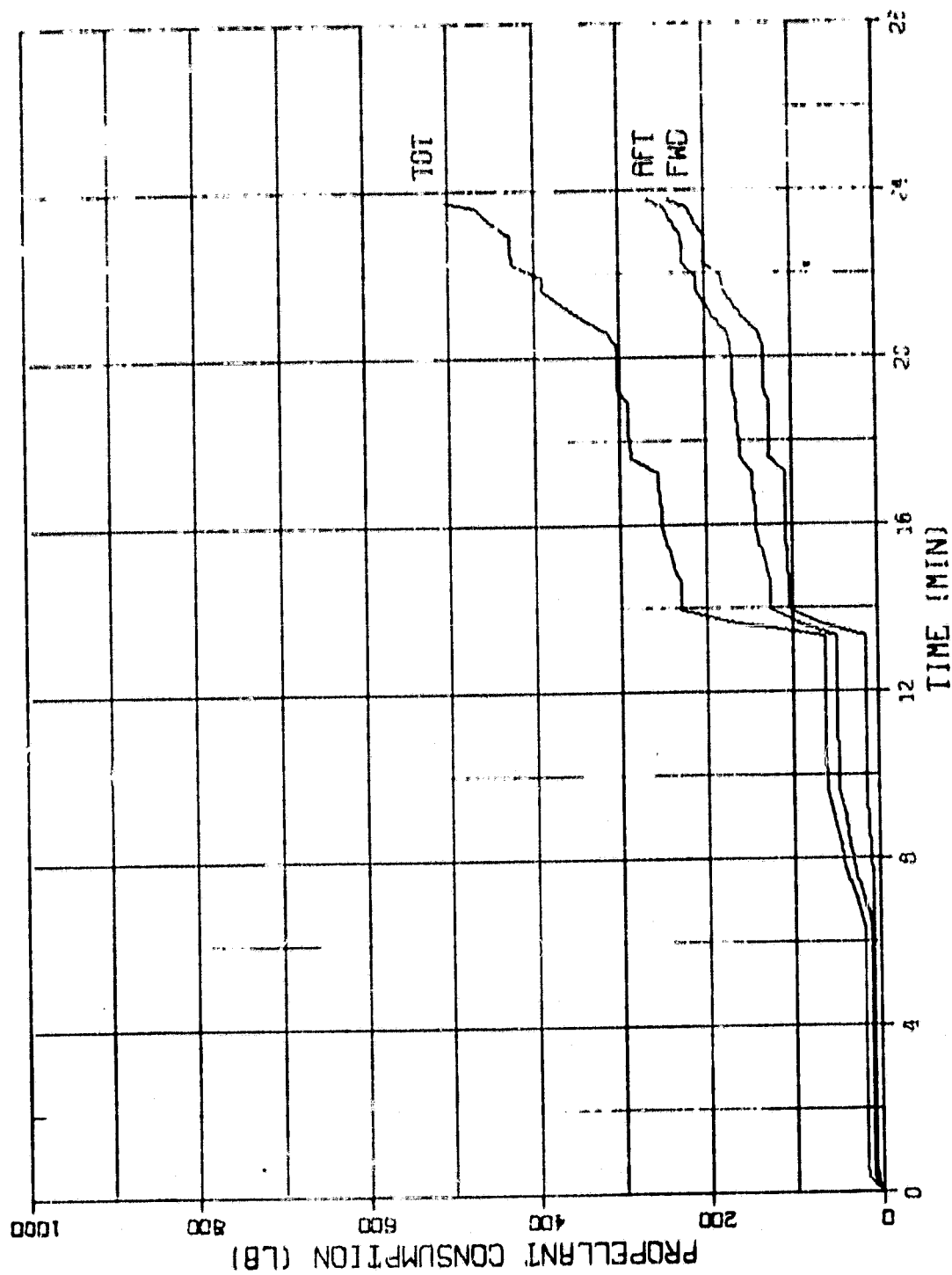


Figure 16.- Propellant consumption (in-plane profile).

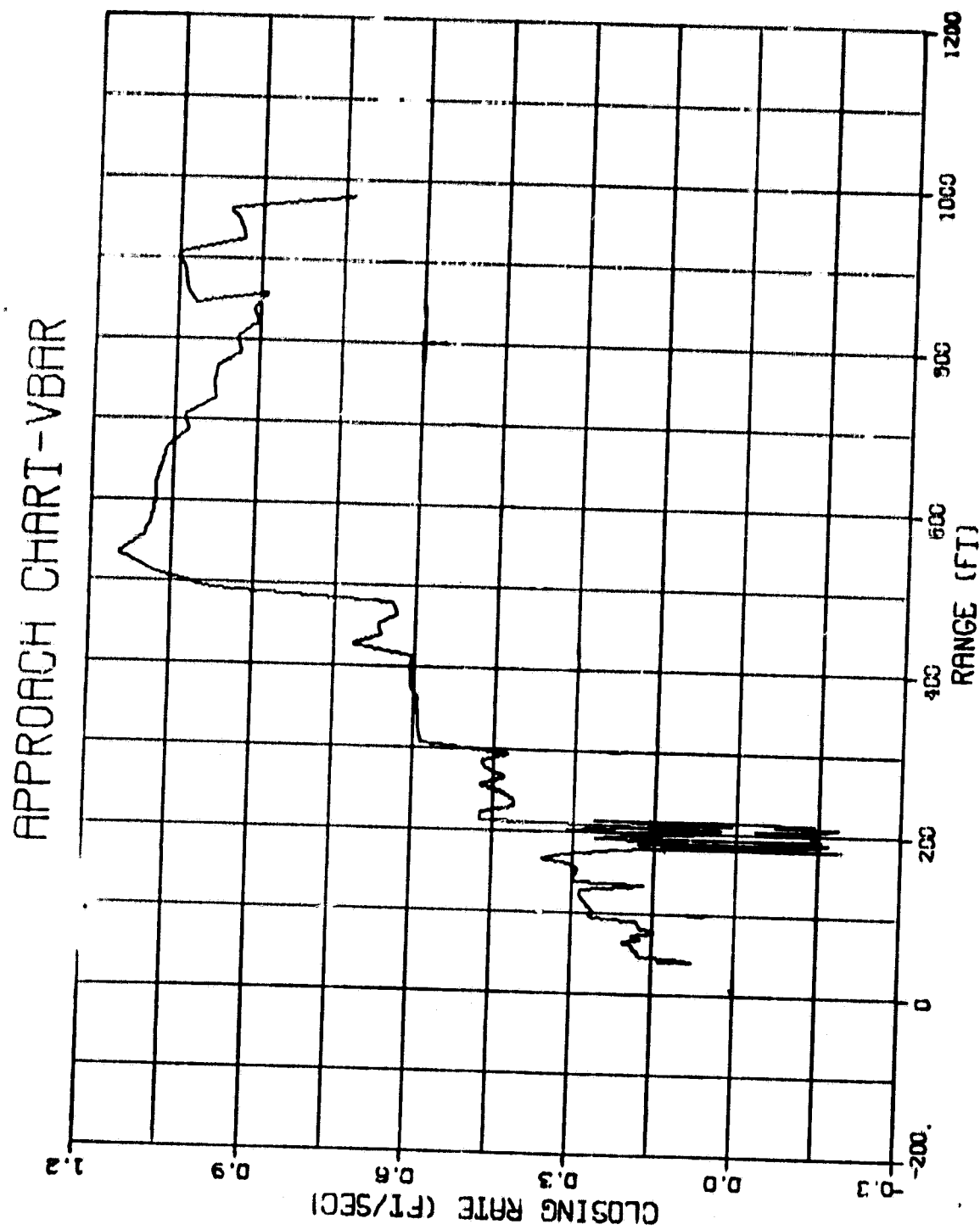


Figure 17.- Approach chart (out-of-plane profile).

ABSOLUTE TORQUE IMPULSE ON PAYLOAD

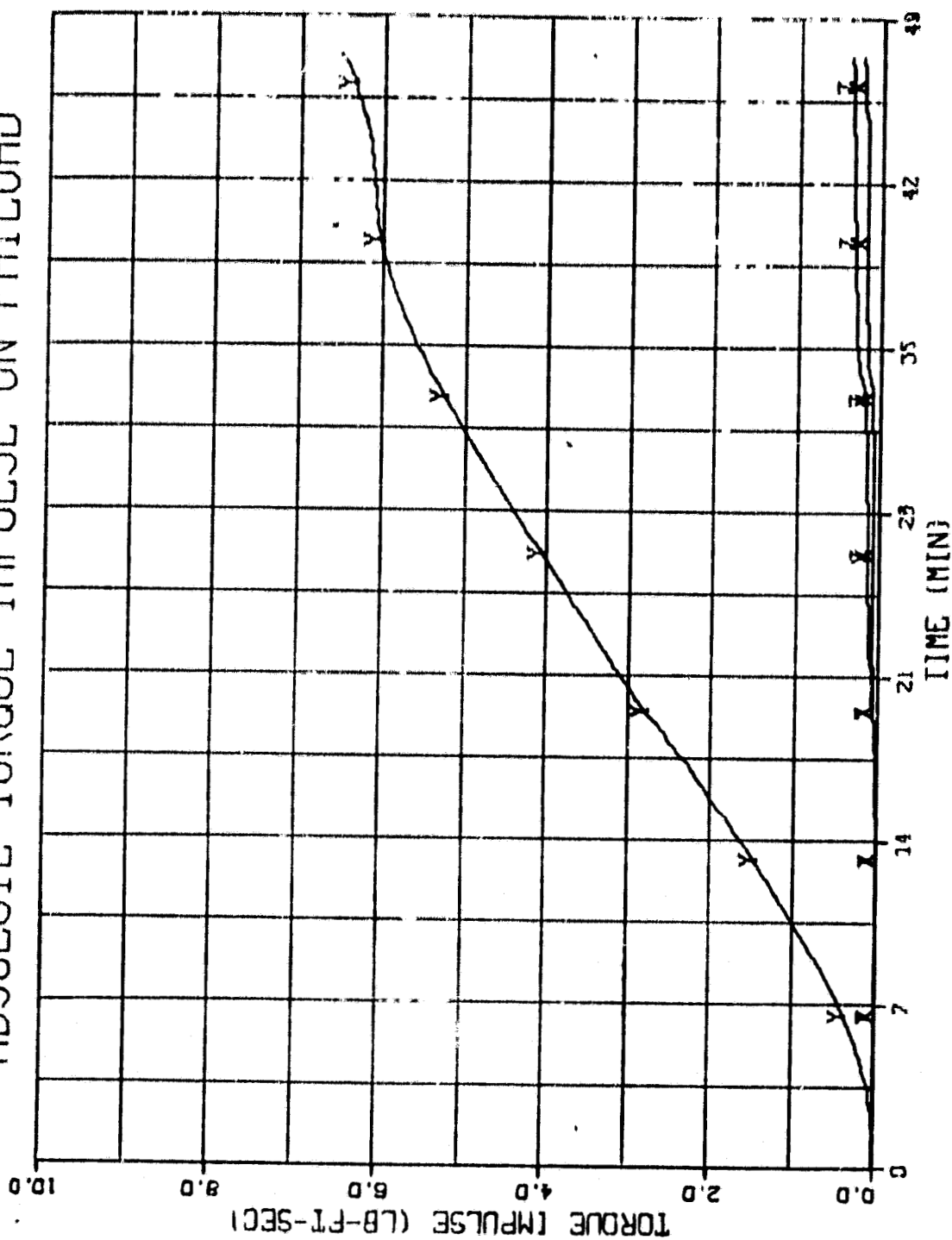


Figure 18.- Torque impulse history (out-of-plane profile).

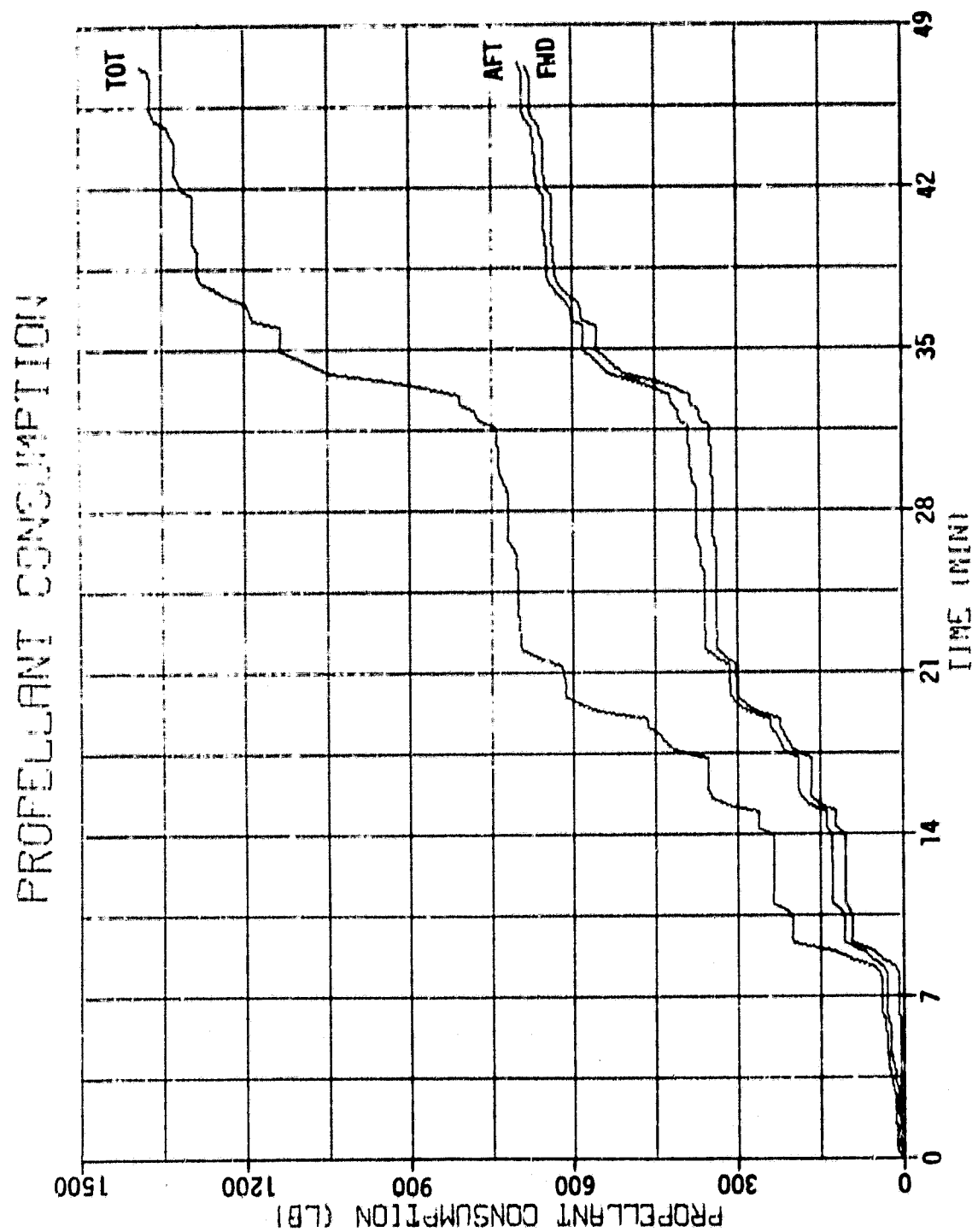


Figure 19.- Propellant consumption (out-of-plane profile).

VIEW FROM ABOVE - VBAR

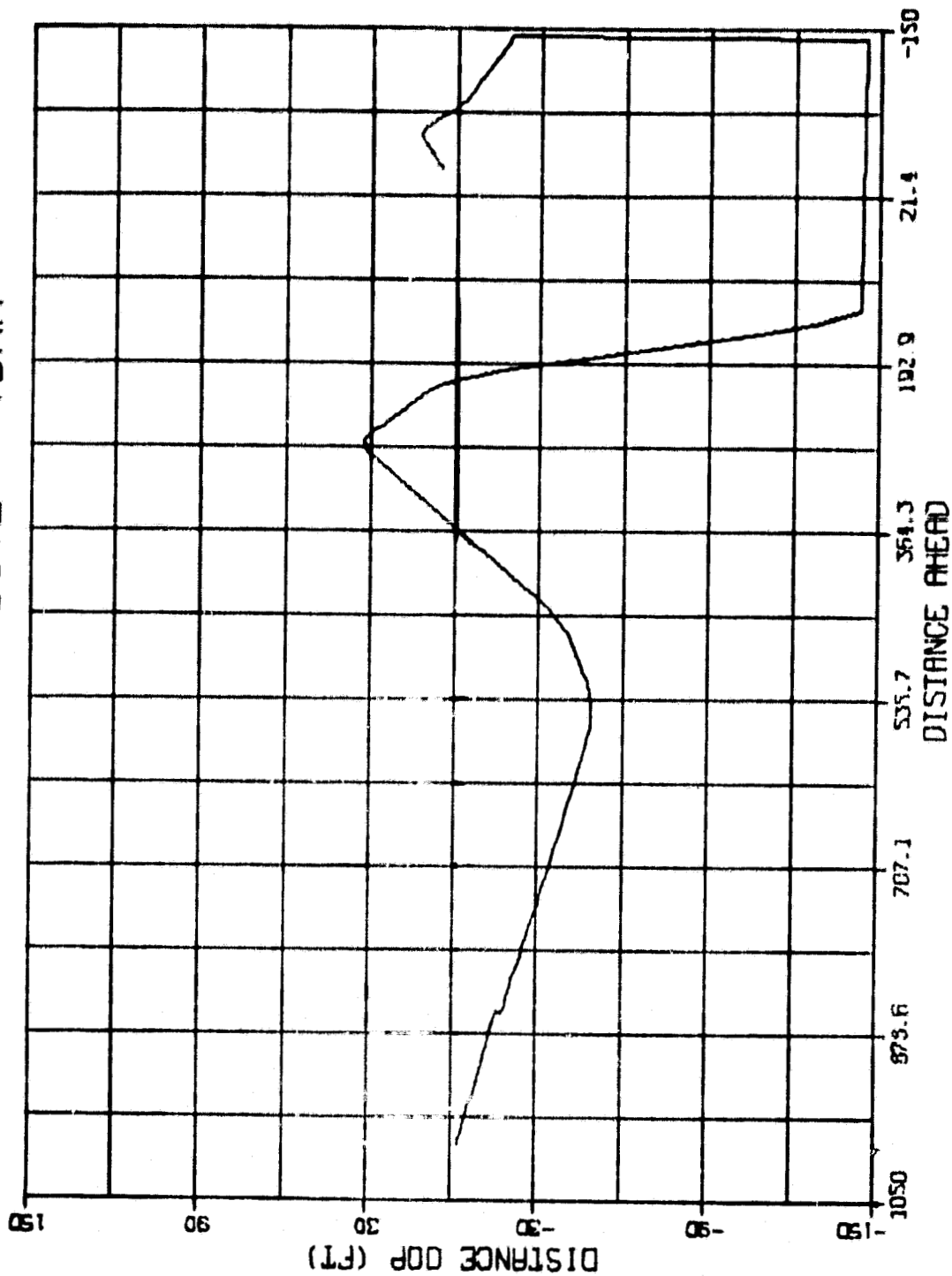


Figure 20.- Third-person view (out-of-plane profile).